

AperTO - Archivio Istituzionale Open Access dell'Università di Torino

**The proapoptotic activity of the Interferon-inducible gene IFI16 provides new insights into its etiopathogenetic role in autoimmunity.**

**This is the author's manuscript**

*Original Citation:*

*Availability:*

This version is available <http://hdl.handle.net/2318/82202> since

*Published version:*

DOI:10.1016/j.jaut.2010.04.001

*Terms of use:*

Open Access

Anyone can freely access the full text of works made available as "Open Access". Works made available under a Creative Commons license can be used according to the terms and conditions of said license. Use of all other works requires consent of the right holder (author or publisher) if not exempted from copyright protection by the applicable law.

(Article begins on next page)



## UNIVERSITÀ DEGLI STUDI DI TORINO

This Accepted Author Manuscript (AAM) is copyrighted and published by Elsevier. It is posted here by agreement between Elsevier and the University of Turin. Changes resulting from the publishing process - such as editing, corrections, structural formatting, and other quality control mechanisms - may not be reflected in this version of the text. The definitive version of the text was subsequently published in [*Journal of autoimmunity* , 35(2), 2010, [10.1016/j.jaut.2010.04.001](https://doi.org/10.1016/j.jaut.2010.04.001) ].

You may download, copy and otherwise use the AAM for non-commercial purposes provided that your license is limited by the following restrictions:

- (1) You may use this AAM for non-commercial purposes only under the terms of the CC-BY-NC-ND license.
- (2) The integrity of the work and identification of the author, copyright owner, and publisher must be preserved in any copy.
- (3) You must attribute this AAM in the following format: Creative Commons BY-NC-ND license (<http://creativecommons.org/licenses/by-nc-nd/4.0/deed.en>), [+ *Digital Object Identifier link to the published journal article on Elsevier's ScienceDirect® platform*]

**The proapoptotic activity of the Interferon-inducible gene IFI16 provides new insights into its etiopathogenetic role in autoimmunity**

Francesca Gugliesi<sup>a</sup>, Marco De Andrea<sup>a,b</sup>, Michele Mondini<sup>b,c</sup>, Paola Cappello<sup>d</sup>, Mirella Giovarelli<sup>d</sup>, Yehuda Shoenfeld<sup>e</sup>, PierLuigi Meroni<sup>f</sup>, Marisa Gariglio<sup>b</sup>, Santo Landolfo<sup>a, \*</sup>

<sup>a</sup> Department of Public Health and Microbiology, University of Turin, Via Santena, 9 – 10126 Turin, Italy; <sup>b</sup> Department of Clinical and Experimental Medicine, Medical School of Novara, Via Solaroli, 17 – 28100 Novara, Italy; <sup>c</sup> NoToPharm SrL, Bioindustry Park del Canavese, Via Ribes , 5 – 10100 Colleterto Giacosa - Turin, Italy; <sup>d</sup> Department of Medicine and Experimental Oncology, and Center for Experimental Research and Medical Studies, University of Turin, 10126 Turin, Italy; <sup>e</sup> Center for Autoimmune Diseases, Sheba Medical Center, Tel Hashomer, Israel; <sup>f</sup> Division of Rheumatology, University of Milan, Istituto G Pini & Istituto Auxologico Italiano, Milan -Italy.

**\*Corresponding author:** Santo Landolfo, Department of Public Health and Microbiology, University of Turin, Via Santena 9, 10126 Turin, Italy. Tel: +390116705636; Fax: +390116705648; E-mail: [santo.landolfo@unito.it](mailto:santo.landolfo@unito.it)

**Abstract**

Several lines of evidence link Interferons (IFNs) autoimmune disorders. Autoantibodies against the Interferon-inducible IFI16 protein, a member of the HIN-200 family constitutively expressed in endothelial cells and keratinocytes, have been identified in patients affected by autoimmune diseases including Systemic Lupus Erythematosus (SLE), Sjogren Syndrome (SjS), and Scleroderma (SSc). These findings point to a role for IFI16 in the etiopathogenesis of autoimmune diseases, but the exact mechanisms involved in the development of autoimmunity remain obscure. In this study, we report for the first time that endothelial cells overexpressing IFI16 undergo apoptosis via the activation of caspase 2 and caspase 3, and that a positive feedback loop appears to link these two caspases. The relevance of IFI16-mediated apoptosis is highlighted by the observation that IFI16 knock down by RNA interference in endothelial cells inhibits the activation of both caspase 2 and caspase 3 by IFN- $\beta$  priming and synthetic double-stranded RNA treatment. Expression of a dominant-negative mutant of IKK2 kinase or treatment with AS602868, an inhibitor of IKK2 activity, results in a strong reduction of NF- $\kappa$ B activation along with absence of caspase 2 and caspase 3 activation and apoptosis induction. Collectively, our findings provide new insights into the role of IFI16 in the pathogenesis of autoimmune diseases by demonstrating that in addition to the stimulation of pro-inflammatory molecules, IFI16 also leads to apoptosis in endothelial cells.

**Keywords:** IFI16, apoptosis, caspase 2/3, NF- $\kappa$ B, interferons, autoimmunity.

## 1. Introduction

Apoptosis or programmed cell death is a fundamental developmental process in animals and plants essential for the regulation and maintenance of tissue growth and homeostasis [1,2]. A number of investigations, ranging from animal models to human pathology, support the view that apoptosis plays an important role in the development of autoimmunity [3-6]. Under normal circumstances apoptotic cells are rapidly cleared by macrophages, “non-professional” phagocytes in the surrounding tissues, and dendritic cells (DC) [7]. This clearance process is, in general, non-inflammatory and may even result in active tolerance towards autoantigens. Defects in this clearance process and the microenvironment in which it occurs may affect the way in which these autoantigens are presented and ultimately result in autoimmunity [8,9]. Moreover, recent data have demonstrated the presence of autoantigens within apoptotic bodies and show that apoptotic cells are critical for antigen presentation [10-12], activation of innate immunity and regulation of cytokine secretion by macrophages [13]. Apoptotic bodies have even been described as “B cell autoantigens” [14].

Interferons (IFNs) are known to have a multitude of immunological functions in both innate and adaptive immunity. Given their pleiotropic effects upon the immune system, it is conceivable that excess quantities of type I IFN or aberrant regulation of its signaling could contribute towards autoimmunity. Several lines of evidence link IFNs with autoimmune disorders, in particular with Systemic Lupus Erythematosus (SLE), Sjogren Syndrome (SjS), and Systemic Sclerosis (SSc) [15, 16]. The expression of a spectrum of genes which constitutes an “IFN signature” is the most significant line of evidence indicating that IFNs may be the dominant pathogenic mediators involved in at least some autoimmune diseases [17,18].

HIN200 comprises a family of structurally related IFN-inducible genes, of which both human (IFI16, IFIX, MNDA, and AIM2) and mouse (Ifi202a, Ifi202b, Ifi203, Ifi204, D3/Ifi205 and Ifi210/AIM2) genes have been sequenced [19-22]. The encoded proteins are primarily nuclear

phosphoproteins involved in the transcriptional regulation of genes that are important for cell cycle control, differentiation, immunomodulation, and apoptosis [23-26].

Immunohistochemical analysis in normal human tissues has revealed prominent IFI16 expression in stratified squamous epithelia, particularly intense in basal cells in the proliferating compartments, whereas it gradually decreased in a more differentiated suprabasal compartment. In addition, endothelial cells from vascular and lymph vessels have been found to strongly express IFI16 [27,28]. This physiological expression of IFI16 in endothelial cells and stratified squamous epithelia (both of which are targets for the clinical manifestations of autoimmune diseases) indicates that IFI16 may be involved in the early steps of inflammation. In support of this hypothesis, overexpression of IFI16 in primary human umbilical vein endothelial cells (HUVEC) efficiently suppressed tube morphogenesis *in vitro* and increased the expression of pro-inflammatory molecules [29,30]. In addition, autoantibodies against the IFN-inducible IFI16 protein have been detected in patients suffering from SLE, SjS, and SSc suggesting an abnormal IFI16 presentation to the afferent limb of the immune system [31].

Since the role of HIN-200 genes in programmed cell death is widely accepted, IFI16 overexpression in apoptotic cells as a further trigger for autoimmunity has been suggested [31]. However, the molecular pathways underlying endothelial cell apoptosis have remained elusive. In particular, it is unknown whether IFI16-mediated apoptosis is dependent on caspase activation. If it is, then it will be important to identify the nature of the initiator and executioner caspases and transduction signals that lead to caspase activation.

In this study, a systematic analysis of the signal transduction pathways upregulated by IFI16 as endothelial cells approach apoptosis upon treatment with Interferon type I (IFN- $\beta$ ) and synthetic double-stranded RNA was performed. Consistent with previous studies, the pathway involving NF- $\kappa$ B, caspase 2, and caspase 3 appeared to play a critical role in IFI16-mediated apoptosis.

## 2. Materials and Methods

### 2.1. Cells lines and reagents

Human umbilical vein endothelial cells (HUVEC) obtained by trypsin treatment of umbilical cord veins were cultured in endothelial growth medium (EGM-2, Lonza, Basel, Switzerland) containing 2% fetal bovine serum (FBS) (Sigma, Milan, Italy), human recombinant vascular endothelial growth factor (VEGF), basic fibroblast growth factor (bFGF), human epidermal growth factor (hEGF), insulin growth factor (IGF-1), hydrocortisone, ascorbic acid, heparin, gentamycin, and amphotericin B, (1 $\mu$ g/ml each; all from Sigma), then seeded into 100-mm culture dishes coated with 0.2% gelatin. Experiments were performed with cells between passages 2-6. Human embryo kidney 293 cells (HEK-293, Microbix Biosystems Inc., Toronto, Canada) were cultured in MEM (Invitrogen, Milan, Italy) supplemented with 10% FBS, 2mM glutamine, 100U/ml penicillin, and 100 $\mu$ g/ml streptomycin sulfate (Sigma). Cells were kept in logarithmic growth phase by 1X Citric Saline detachment and replating every 2-4 days. AS602868 is an anilino-pyrimidine derivative and adenosine triphosphate (ATP) competitor that has been selected for its inhibitory activity *in vitro* on IKK2, the constitutively active form of IKK2 [33,33]. Stocks of AS602868 were prepared in 100% DMSO. In all experiments in which AS602868 was used, each dish of cells received an equal volume of DMSO. When infections were performed in presence of AS602868, the cells were treated with the compound 10h after the infection. Caspase 2 inhibitor Z-Val-Asp(O-Me)-Val-Ala-Asp(O-Me) fluoromethyl ketone (Z-VDVAD-FMK) and caspase 3 inhibitor Z-DEVD-FMK were purchased from Sigma and R&D system, respectively. When infections were performed in presence of caspase 2 or caspase 3 inhibitors, the cells were treated with the compound 1h before the infection. Doxorubicin was purchased from Sigma and was used at 1 $\mu$ M as indicated.

### 2.2. Recombinant adenovirus preparations and HUVEC infection

The pAC-CMV IFI16 containing the human IFI16 cDNA linked to a FLAG-tag at the NH<sub>2</sub>-terminal was co-transfected with pJM17 into human embryonic kidney 293 cells as previously described [34,35]. After several rounds of plaque purification, the adenovirus containing the IFI16

gene (AdVIFI16) was amplified on 293 cell monolayers and purified from cell lysates by banding twice on CsCl gradients. Desalting was performed using G50 columns (GE Healthcare, Milan, Italy), and viruses were frozen in PBS-10% glycerol at -80°C. The infectious titers (PFU) were determined by a standard plaque assay on 293 cell monolayers. The physical particles of the vector preparations were measured by spectrophotometry, and our viral preparations showed a 1:10-1:20 ratio between PFU and physical particles. Endotoxin contamination was excluded by testing with the E-Toxate kit (Sigma, sensitivity >1.4 pg/ml). For cell transduction, pre-confluent HUVEC were washed once with phosphate-buffered saline (PBS) and incubated with AdVIFI16 or AdVLacZ (used as a control) at a multiplicity of infection (MOI) of 300 in EGM-2. After 60 min at 37°C, the virus was washed off and fresh medium was added.

### *2.3. Immunoblotting*

Whole-cell protein extracts were prepared by resuspending pelleted cells in lysis buffer containing 125 mM Tris-Cl (pH 6.8), 1% SDS, 20 mM dithiothreitol, 1 mM phenylmethylsulfonyl fluoride, 4 µg/ml leupeptin, 4 µg/ml aprotinin, and 1 µg/ml pepstatin (all from Sigma). After a brief sonication, soluble proteins were collected by centrifugation at 15,000 x g. Supernatants were analyzed for protein concentration using a Bio-Rad D<sub>c</sub> protein assay kit (Milan, Italy) and stored at -70°C in 10% glycerol. Proteins were separated by SDS-PAGE then transferred to Immobilon-P membranes (Millipore, Milan, Italy). Filters were blocked in 5% non-fat dry milk in 10 mM Tris-Cl (pH 7.5), 100 mM NaCl, and 0.1% Tween 20, and immunostained with rabbit anti-IFI16 Ab (diluted 1:2000) or mouse anti-actin mAb (Chemicon, Milan, Italy) (diluted 1:4000).

### *2.4. In vitro analysis of caspase activities*

Caspase 1, 2, 3, 8, and 9 protease activity was measured in a fluorometric assay, by measuring the extent of cleavage of a fluorometric peptide substrate using SensoLyte AFC Caspase Sampler Kit Fluorimetric (Anaspec, CA, USA). Experiments were performed according to the manufacturer's instructions. After a 1h of incubation at 25°C, fluorescence was measured at an excitation wavelength of 405 nm and an emission wavelength of 500 nm using the VICTOR<sup>3</sup> 1420



multilabel counter (Perkin-Elmer, Milan, Italy). Protease activity was expressed as RFU (relative unit of fluorescence).

### 2.5. Nuclear extract isolation and Electrophoretic Mobility Shift Assay (EMSA)

HUVEC were plated at a density of  $3 \times 10^5$  cells/100-mm diameter dish and 24h later infected with either AdVIFI16 or AdVLacZ, or mock infected. At the indicated times post-infection (hpi), cells were washed in cold PBS and nuclear proteins were extracted using the Nuclear Extract Kit (Active Motif, Carlsbad, CA) according to the manufacturer's instructions. EMSA was performed as previously described [32]. Briefly, nuclear extracts (15  $\mu$ g of protein) were incubated in a binding buffer (10mM Tris-HCl (pH 7.9), 50mM NaCl, 0.5mM EDTA, 1mM dithiothreitol, and 7.5mM MgCl<sub>2</sub>) with 2 $\mu$ g of poly(dI-dC) (GE Healthcare) and <sup>32</sup>P-labeled double-stranded NF-kB consensus oligonucleotides (Promega, Milan, Italy). The oligonucleotide probe was labeled with [ $\gamma$ -<sup>32</sup>P]ATP (GE Healthcare) and T4 polynucleotide kinase according to the manufacturer's protocol and column-purified on G-25 Sephadex (Bio-Rad). Complexes were analyzed by non-denaturing 4% PAGE, the gels dried, and DNA-protein complexes detected by autoradiography.

### 2.6. Real Time RT-PCR analysis

RT-PCR analysis was performed on an Mx 3000P<sup>TM</sup> (Stratagene, Milan, Italy) utilizing SYBR Green I dye (Invitrogen) as a non-specific PCR product fluorescence label. Total cellular RNA was isolated using Eurozol (Euroclone, Milan, Italy). RNA (1  $\mu$ g) then retro-transcribed at 42 °C for 60 min in PCR buffer (1.5 mM MgCl<sub>2</sub>) containing 5  $\mu$ M random primers, 0.5mM dNTP, and 100 units of Moloney murine leukemia virus reverse transcriptase (Applied Biosystems/Ambion, Austin, USA) in a final volume of 20  $\mu$ l. cDNA (2 $\mu$ l) or water (as control) was amplified in duplicate by real time RT-PCR using the Brilliant SYBR Green QPCR master mix (Stratagene) in a final volume of 25 $\mu$ l. Primer sequences were as follows: IFI16 (sense, 5'-ACT GAG TAC AAC AAA GCC ATT TGA-3'; antisense, 5'-TTG TGA CAT TGT CCT GTC CCC AC-3'); ICAM-1 (sense, 5'-CAA CCG GAA GGT GTA TGA AC-3'; antisense, 5'-CAG CGT AGG GTA AGG TTC-3'); CCL20 (sense, 5'-CCA AGA GTT TGC TCC TGG CT-3'; antisense, 5'-TGC TTG CTG CTT CTG ATT CG-3');

p21 (sense, 5'-CGC TAA TGG CGG GCT G-3'; antisense, 5'-CGG TGA CAA AGT CGA AGT TCC-3') and  $\beta$ -actin (sense, 5'-GTT GCT ATC CAG GCT GTG-3'; antisense, 5'-TGT CCA CGT CAC ACT TCA-3'). For quantitative analysis, semi-logarithmic plots were constructed of  $\Delta$  fluorescence versus cycle number and a threshold set for the changes in fluorescence at a point in the linear PCR amplification phase ( $C_t$ ). The  $C_t$  values for each gene were normalized to the  $C_t$  values for  $\beta$ -actin by means of the  $\Delta C_t$  equation. The level of target RNA, normalized to the endogenous reference and relative to the uninfected and untreated cells, was calculated by the comparative  $C_t$  method with the  $2^{-\Delta\Delta C_t}$  equation.

### 2.7. Small interfering RNA preparation and electroporation

HUVEC cells ( $5 \times 10^5$  cells/well) were electroporated with IFI16 small interfering RNA mix (siRNA) (Hs\_IFI16\_4 HP siRNA, Hs\_IFI16\_6 HP siRNA, Hs\_IFI16\_7 HP siRNA, Hs\_IFI16\_8 HP siRNA; Qiagen) to give a final concentration of  $1.25 \mu\text{M}$  by using MicroPorator MP-100 (Digital BioTechnology, Seoul, Korea), according to the manufacturer's instructions. At 48h after transfection, cells were treated with human IFN- $\beta$  for 24h ( $1000 \text{ IU/ml}$ ) (Sigma) and then for 5h or 12h with synthetic double-stranded RNA (dsRNA) (poly rI:rC,  $50 \mu\text{g/ml}$ ) (Invitrogen). AllStars Negative Control siRNA (Qiagen) was used as non-specific siRNA. For cell transduction, HUVEC cells electroporated with Hs\_CASP2\_10 HP or Hs\_CASP3\_7 HP validated small interfering RNA mix were washed once with phosphate-buffered saline (PBS) and incubated with AdvIFI16 or AdvLacZ (used as a control) at a MOI of 300 in EGM-2. After 60 min at  $37^\circ\text{C}$ , the virus was washed off and fresh medium added.

### 2.8. Annexin V analysis

To distinguish apoptotic from necrotic cells, double staining for exposed phosphatidylserine and propidium iodide (PI) exclusion was performed using the Annexin V-FITC Apoptosis Detection Kit (Calbiochem, Milan, Italy). Experiments were performed according to the manufacturer's instructions. Cells were analyzed utilizing a FACSCalibur (BD Biosciences). Controls of unstained

cells, cells stained with Annexin V-FITC only, or cells stained with PI only were used to establish compensation and quadrants. Cells were gated according to their light-scattering properties to exclude cell debris.

### 2.9. TUNEL staining

DNA damage was evaluated and quantified using a colorimetric apoptosis detection kit (Titer TACS; Trevigen) and TUNEL stain in a 96-well format following the manufacturer's instructions. Briefly, cells were cultured in 96-well plates and left uninfected, or infected with AdVLacZ or AdvIFI16, or treated with doxorubicin (1 $\mu$ M). At 48hpi, cells were fixed with 3.7% buffered formaldehyde for 5 min, washed once with PBS, permeabilization with 100% methanol for 20 min and subsequently washed once with PBS. Cells were then subjected to a labeling procedure following the manufacturer's instructions. Absorbance was measured at 450 nm using the VICTOR<sup>3</sup> 1420 multilabel counter (Perkin-Elmer, Milan, Italy). Data are expressed as % of Positive Control (DNase treated cells), according to the formula:  $(\text{Sample OD value} - \text{blank}) / (\text{Positive Control OD value} - \text{blank}) \times 100$ .

### 2.10. Cell cycle analysis

Cell cycle analysis was performed by PI staining of DNA. Briefly, cells were harvested and fixed in 50% cold ethanol for 60 min at 4°C, washed twice with PBS, incubated at 37°C in citrate buffer (0.05M Na<sub>2</sub>HPO<sub>4</sub>, 25mM sodium citrate, and 0.1% Triton X-100, pH 7.8), and stained with 100  $\mu$ g/ml PI for 30 min (for dye stabilization) in the presence of RNase (100 ng/ml). Cellular DNA content was then assessed utilizing a FACSCalibur flow cytometer (BD Biosciences) and analyzed with the ModFit LT software program (BD Biosciences).

### 2.11. Statistical analysis

All statistical analyses and graphs were performed using GraphPad Prism version 4.03 for Windows (GraphPad Software, San Diego California USA, [www.graphpad.com](http://www.graphpad.com)). The data were presented as the means  $\pm$  standard deviations (SD) and analyzed with one-way ANOVA followed by Bonferroni post-test.

### 3. Results

#### *3.1. IFI16 inactivation prevents apoptosis induced by IFN- $\beta$ priming followed by dsRNA treatment.*

In search for a model that allowed us to assess the physiological impact of IFI16 in apoptosis induction, the capability of endogenous IFI16 as mediator of IFN-I-induced apoptosis upon treatment with dsRNA of endothelial cells was investigated [36]. It was found that dsRNA is indeed able to induce apoptosis in HUVEC, and that priming the cells with IFN-type I reduces the time between first contact with dsRNA and the initiation of apoptosis. As IFN-type I priming followed by the addition of dsRNA is able to activate a variety of different caspases, we decided to exploit this model in order to evaluate the ability of endogenously-stimulated IFI16 to selectively control caspase 2 and 3 activities.

Endogenous IFI16 was depleted by electroporating HUVEC with specific siRNA and its expression in HUVEC primed with 1000 IU human IFN- $\beta$  for 24 h and treated with poly rI:rC (50  $\mu$ g/ml) was analyzed. As shown in Fig. 1A, IFN- $\beta$  priming followed by poly rI:rC treatment induced higher levels of IFI16 expression compared to untreated cells. In contrast, electroporation of IFI16-targeted siRNA efficiently blocked endogenous IFI16 expression following the treatment of HUVEC with IFN- $\beta$  and poly rI:rC. Control siRNA-electroporated HUVEC displayed IFI16 levels similar to those observed in cells treated with IFN- $\beta$  and poly rI:rC (Fig. 1A). Next, we assessed IFN- $\beta$  and poly rI:rC induced apoptosis in the absence of IFI16 expression. As shown by the reduced levels of Annexin V binding in Fig. 1B, the lack of IFI16 expression significantly reduced the occurrence of apoptosis in HUVEC primed with IFN- $\beta$  and then challenged with poly rI:rC. No reduction of apoptosis was observed when HUVEC were electroporated with control siRNA and then treated with IFN- $\beta$  and poly rI:rC.

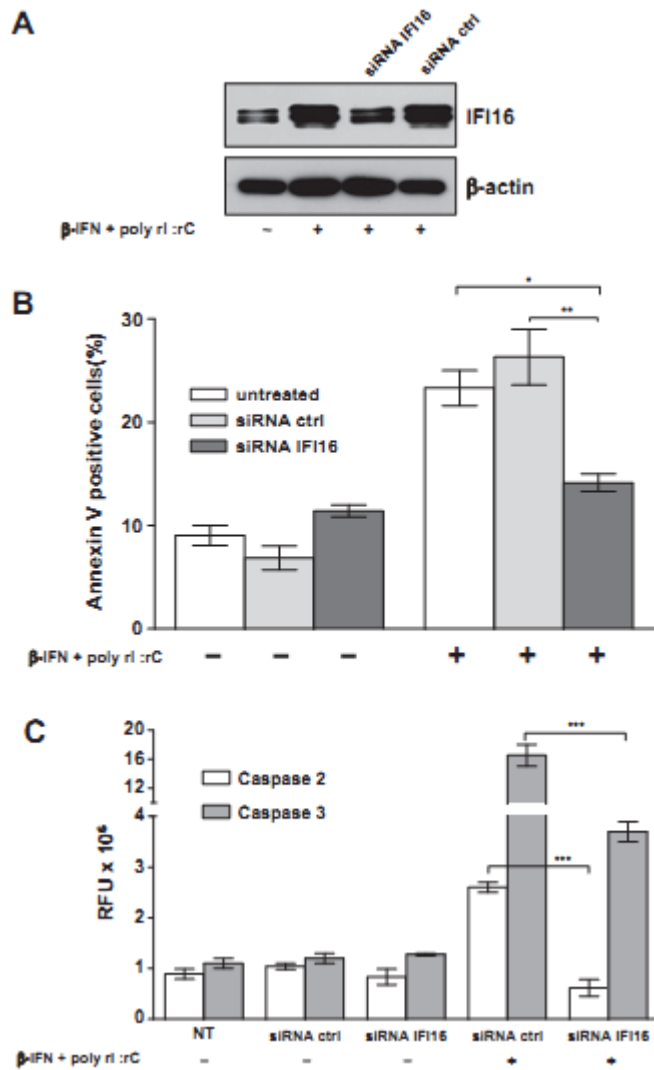


**Fig. 1.** IFI16 inactivation prevents apoptosis induced by IFN- $\beta$  and poly rI:rC treatment. HUVEC electroporated with a specific siRNA-IFI16 mix (siRNA-IFI16) or control siRNA (siRNA ctrl), primed with 1000 IU human IFN- $\beta$  for 24 h and then treated with poly rI:rC (50  $\mu$ g/ml), were analyzed for IFI16 expression (A – 5 h poly rI:rC treatment), Annexin V-FITC binding (B – 12 h poly rI:rC treatment) and caspase activation (C – 5 h poly rI:rC treatment). Data are shown as mean  $\pm$  SD; n = 3. \*P < 0.05, \*\*P < 0.01, \*\*\*P < 0.001 (two-way ANOVA).

As priming with IFN-type I followed by poly rI:rC treatment non-selectively stimulates the activation of the various different caspases [36], this model offers the possibility to assess the capability of IFI16 to specifically down-regulate the activity of caspases 2 and 3 out of the different caspases activated by IFN-type I and poly rI:rC. As shown in Fig. 1C, in treated HUVEC

electroporated with siRNA specific for IFI16, the activation of both caspase 2 and caspase 3 was significantly down-regulated compared to the levels of activation observed in treated HUVEC electroporated with control siRNA. In contrast, in HUVEC electroporated with IFI16-siRNA and HUVEC electroporated with control siRNA, the activation of caspases 8 and 9 appeared to be completely unaffected (data not shown).

Altogether, these results demonstrate that IFI16 selectively regulates the activation of caspases 2 and 3, and contributes to the regulation of apoptosis triggered by IFN-type I priming followed by dsRNA treatment.

### *3.2. IFI16 inhibits cell growth and angiogenesis by triggering apoptosis*

To confirm that IFI16 overexpression is sufficient to induce caspase activation and apoptosis, HUVEC infected with AdvIFI16, AdvLacZ, or left uninfected were then analyzed for apoptotic features using the following combination of cell death classification methods [37]: i) analysis of sub-G1 occurrence, ii) Annexin V/propidium iodide FACS sorting, and iii) TUNEL assay. As demonstrated in the flow cytometric histogram profile depicted in Fig. 2A, uninfected and AdvLacZ-infected HUVEC displayed similar percentages of cells in G1 (65% vs. 62%), S (13% vs. 13%), and G2/M (18% vs. 21%) phases. In both cell cultures, only a minor fraction of cells presented DNA content less than 2N – a feature indicative of apoptosis. In stark contrast, AdvIFI16-infected HUVEC displayed a significant increase in the subdiploid (sub-G1) population (18%) accompanied by a decrease in cell fractions accumulated in G1 (44%) and S (9%) phases. The G2/M population was only slightly increased (26%). Since an increase in cells with sub-G1 DNA content is indicative of apoptosis, we decided to confirm our results via Annexin V/propidium iodide FACS sorting. As shown in Fig. 2B, uninfected and AdvLacZ-infected cells displayed similar percentages of apoptotic cells. In contrast, AdvIFI16-infected cultures contained, on the average, 50% total apoptotic cells, which is 5-fold higher than in the AdvLacZ-infected cells ( $P < 0.001$ ). Similar results were obtained using the quantitative (TiterTACS) TUNEL assay (Fig. 2C).

After infection with AdVIFI16 or treatment with doxorubicin, HUVEC displayed DNA damage as shown by positive TUNEL staining (45% and 67% respectively). In contrast, HUVEC left uninfected or infected with AdVLacZ showed low levels of positive TUNEL staining, indicating that the DNA breaks detected by TUNEL were specifically induced by IFI16. As expected, cell cultures treated with doxorubicin displayed high levels of positive TUNEL staining (Fig. 2C).

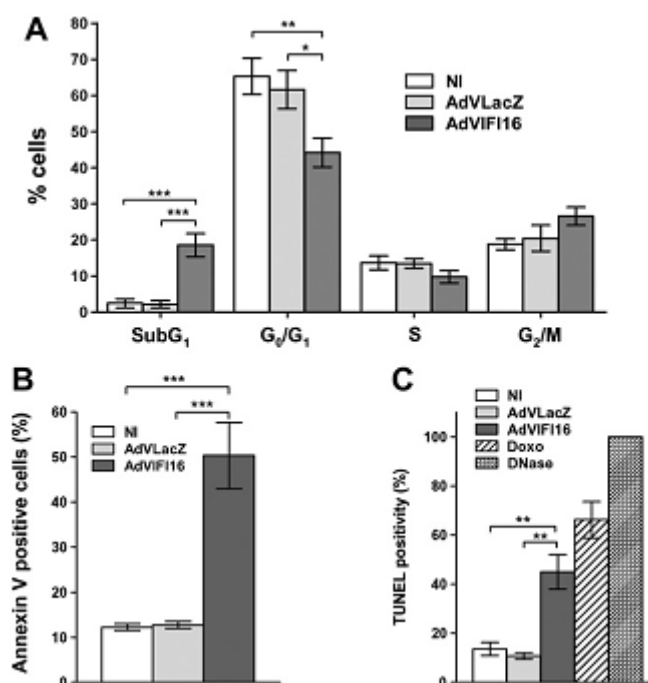


**Fig. 2.** IFI16-induced cell death in normal primary endothelial cells (HUVEC). (A) HUVEC were left untreated (NI), or infected with AdVLacZ or AdVIFI16. At 48 hpi cells were stained with propidium iodide (PI) and analyzed for cell cycle distribution and appearance of sub-G1 nuclei by flow cytometry. Data are shown as mean  $\pm$  SD; n = 3. \*P < 0.05, \*\*P < 0.01, \*\*\*P < 0.001 (one-way ANOVA). (B) HUVEC were left uninfected (NI), or infected with AdVLacZ or AdVIFI16. At 48 hpi, cells were stained with Annexin V-FITC and PI and analyzed by flow cytometry. Data are shown as mean  $\pm$  SD; n = 3. \*\*\*P < 0.001 (one-way ANOVA). C. At 48 hpi DNA damage in HUVEC cells left uninfected (NI), infected with AdVIFI16 or AdVLacZ or treated with doxorubicin (1  $\mu$ M) was evaluated and quantified using a colorimetric apoptosis detection kit (Titer TACS; Trevigen) at 48 hpi. For comparison, data are expressed as % of the positive control

(DNase treated cells) according to the formula: (Sample OD value-blank)/(Positive Control OD value-blank)  $\times$  100. Data are shown as mean  $\pm$  SD; n = 3. **\*\*P** < 0.01 (one-way ANOVA).

### 3.3. Caspase 2 is required for IFI16-induced cell death

Current models of apoptosis stipulate that a specific hierarchy of caspase activation regulates its induction, whereby a variety of apoptotic signals are responsible for first activating the initiator caspases that subsequently target effector or executioner caspases, such as caspase 3 [39]. To identify the caspases that might participate in IFI16-induced apoptosis, HUVEC were infected with AdvIFI16, AdvLacZ, or left uninfected for 24h, 48h, and 72h. Cytosolic caspase activity was analyzed by degrading fluorogenic substrates specific for caspases 1, 2, 8, and 9 in order to investigate the initiator caspase(s) involved, and by degrading a fluorogenic caspase 3 specific substrate in order to study the involvement of this executioner caspase. As shown in Fig. 3, IFI16 overexpression augmented both caspase 2 and 3 activities as early as 48h, and sustained levels persisted until at least 72h after infection. In contrast, the activity of caspases 1, 8, and 9 activities were not affected by AdvIFI16 infection at any time point tested (data not shown). Moreover, as infection with AdvLacZ did not trigger any increase in activity in any of the caspases studied as no caspase activity was observed in the uninfected HUVEC, we can deduce that activation of caspases 2 and 3 was specific for IFI16 under these conditions.

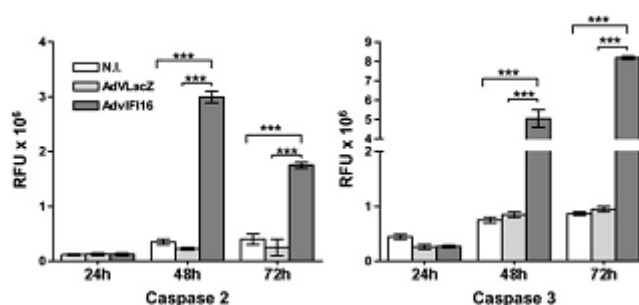


**Fig. 3.** IFI16 activates both caspase 2 and caspase 3 in endothelial cells. Cells were left uninfected (NI), or infected with AdvLacZ or AdvIFI16. At the indicated time points, cells were harvested and identical amounts of cytosolic proteins were used in a fluorogenic caspase assay by measuring



the extent of cleavage of a fluorometric peptide substrate. The protease activity was expressed as RFU (relative unit of fluorescence). Data are shown as mean  $\pm$  SD; n = 3. \*\*\*P < 0.001 (two-way ANOVA).

Two different approaches have been used to date to probe the biological role of caspases: i) the pharmacological blockade of caspase activity during situations in which caspases are activated, and ii) diminishing the cellular levels and activities of caspases by means of RNA interference [1,2]. Both techniques were used in the present study. In order to evaluate the effects of caspase 2 and 3 inhibitors on IFI16-mediated apoptosis, HUVEC were infected with AdVIFI16 or AdVLacZ, treated with doxorubicin (as a positive control of apoptosis induction), or left untreated, then incubated in the presence or absence of the appropriate caspase 2 and 3 inhibitors. The activation of caspase 2 and caspase 3, and apoptosis induction via Annexin V/propidium iodide FACS sorting were then analyzed. As shown in Fig. 4A, IFI16 overexpression significantly increased the activity of both caspases to levels that were comparable to those observed in AdVLacZ-infected and uninfected (NI) HUVEC. Treatment with doxorubicin, known to increase caspase 2 and 3 activities [40], was similarly inhibited by the specific inhibitor. In line with the results of the caspase activity measurements, Annexin V/propidium iodide FACS sorting showed that treating AdVIFI16-infected cells with caspase 2 and 3 inhibitors reduced the levels of apoptosis to levels comparable to those observed in uninfected or AdVLacZ-infected cells (Fig. 4B).

To definitively confirm the involvement of caspase 2 and caspase 3 in IFI16-induced apoptosis, their corresponding genes were silenced through the use of specific siRNAs. As shown in Fig. 3C, knock down of caspase 2 expression inhibited IFI16-induced activation of both caspase 2 and 3. Interestingly, knock down of the caspase 3 gene reduced its activity by about 60%, whereas caspase 2 was only partially decreased.

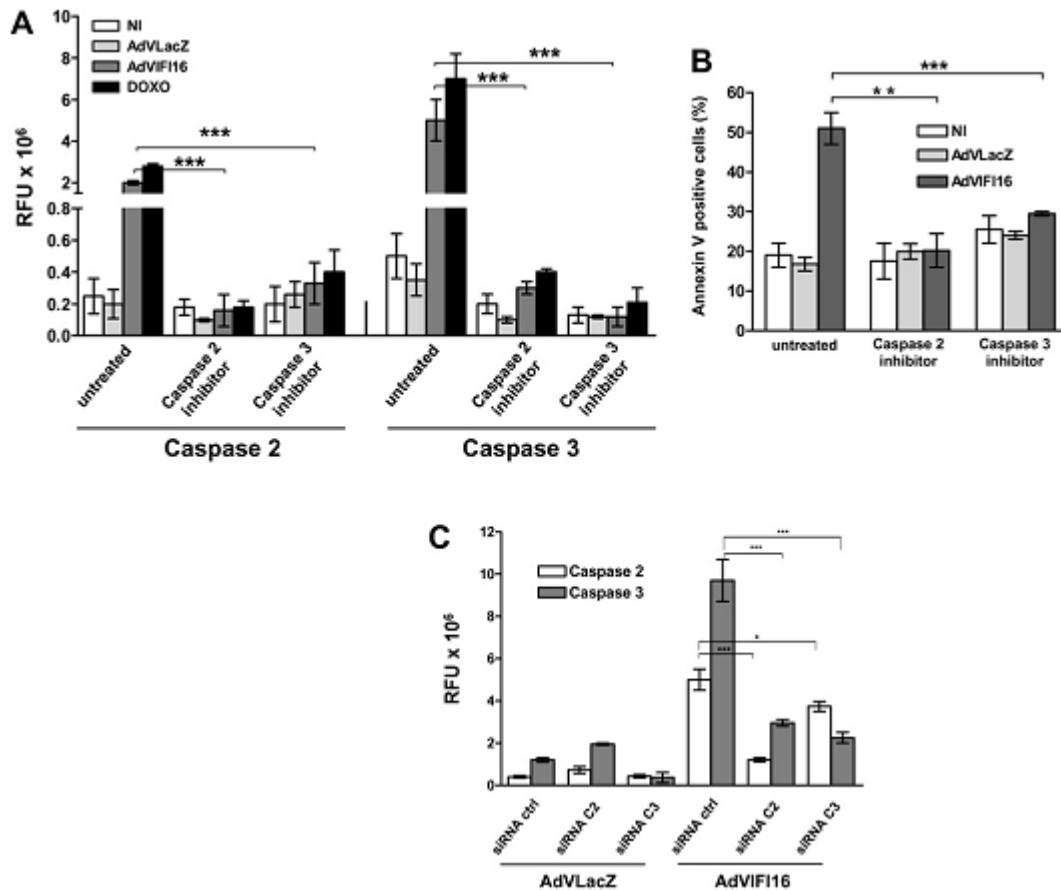


**Fig. 4.** Activation of both caspase 2 and caspase 3 is necessary for full apoptotic effect. HUVEC were left uninfected (NI), infected with AdVLacZ or AdVIFI16, or doxorubicin-treated in the presence or absence of the caspase 2 inhibitor Z-VDVAD-FMK or caspase 3 inhibitor Z-DEVD-FMK (50  $\mu$ M). At 48 hpi, the activation of caspase 2 and caspase 3 was analyzed in cell extracts (A), while other cells were stained with Annexin V-FITC and PI and analyzed by flow cytometry (B). (C) HUVEC electroporated with either Hs\_CASP2\_10 HP or Hs\_CASP3\_7 HP siRNA or control siRNA (siRNA ctrl), were left uninfected (NI), or infected with either AdVLacZ or AdVIFI16. At 48 hpi, the activation of caspase 2 and caspase 3 was measured. In A and C, the protease activity was expressed as RFU (Relative Fluorescence Unit). Data are shown as mean  $\pm$  SD; n = 3. \*P < 0.05, \*\*P < 0.01, \*\*\*P < 0.001 (two-way ANOVA).

Collectively, these findings indicate that: i) IFI16-induced apoptosis is mediated through the simultaneous activation of both caspase 2 and caspase 3, ii) the activation of caspase 3 depends on

caspase2, although a positive feedback loop from caspase 3 to 2 may also exist, and iii) in the absence of caspase 3, caspase 2 behaves as an effector caspase triggering endothelial cell apoptosis.

#### 3.4. IFI16-driven induction of apoptosis depends on the NF- $\kappa$ B complex

We recently demonstrated that NF- $\kappa$ B was the main mediator of pro-inflammatory molecule induction by IFI16 in endothelial cells [30]: NF- $\kappa$ B activation was found to be triggered by IFI16 through a novel mechanism involving the suppression of I $\kappa$ B $\alpha$  promoter transcription that was accompanied by the down-regulation of I $\kappa$ B $\alpha$  mRNA and protein expression. As a consequence, NF- $\kappa$ B heterodimers composed of p50 and p65 freely translocated into the nucleus transactivating NF- $\kappa$ B dependent genes, including ICAM-1, CCL20, and MCP1.

To examine whether the NF- $\kappa$ B pathway was also involved in IFI16-induced apoptosis, the activation status of NF- $\kappa$ B was evaluated by analyzing the IKK2 subunit. In order to do so, a recombinant adenoviral vector was used to introduce a mutated IKK2 protein into HUVEC cells; the mutant IKK2 bore a Lys to Ala point mutation at position 44 that inhibits the activity of its endogenous counter-partner [32] and [33]. This substitution abolishes IKK2 protein kinase activity and gives the vector a dominant-negative phenotype (dnIKK2). A multiplicity of infection (MOI) of 100 was used to achieve dnIKK2 expression in 90–100% of HUVEC [34]. To characterize the effects of dnIKK2 on IFI16-mediated apoptosis, HUVEC infected with AdVLacZ, AdvIFI16, or left uninfected were infected 4 h later with either AdvdnIKK or AdVLacZ and 48 h later analyzed for the activation of caspases 2 and 3 and assessed for Annexin V/propidium iodide FACS sorting. Under these culture conditions, the expression of dnIKK resulted in a strong reduction of I $\kappa$ B $\alpha$  degradation and NF- $\kappa$ B activation without impairing IFI16 expression (data not shown). As shown in Fig. 5A, infection of endothelial cells with AdvdnIKK2, leading to NF- $\kappa$ B inactivation, prevented the induction of IFI16-triggered caspase 2 and caspase 3 activities. In contrast, IFI16 overexpression followed by AdVLacZ infection triggered high levels of caspase 2 and 3 activities

in comparison with cells infected with AdVLacZ alone. In line with the results of caspase activity analyses, overexpression of dnIKK2 in AdVIFI16-infected HUVEC (AdVdnIKK2 + AdVIFI16) resulted in a fraction of total apoptotic cells that was reduced (29%) and similar to that observed in cultures infected with AdVLacZ + AdVdnIKK2 (27%) (Fig. 5B). As expected, IFI16 overexpression in cells infected with AdVIFI16 alone or AdVIFI16 + AdVLacZ displayed an elevated percentage of total apoptotic cells (49% and 46% respectively).

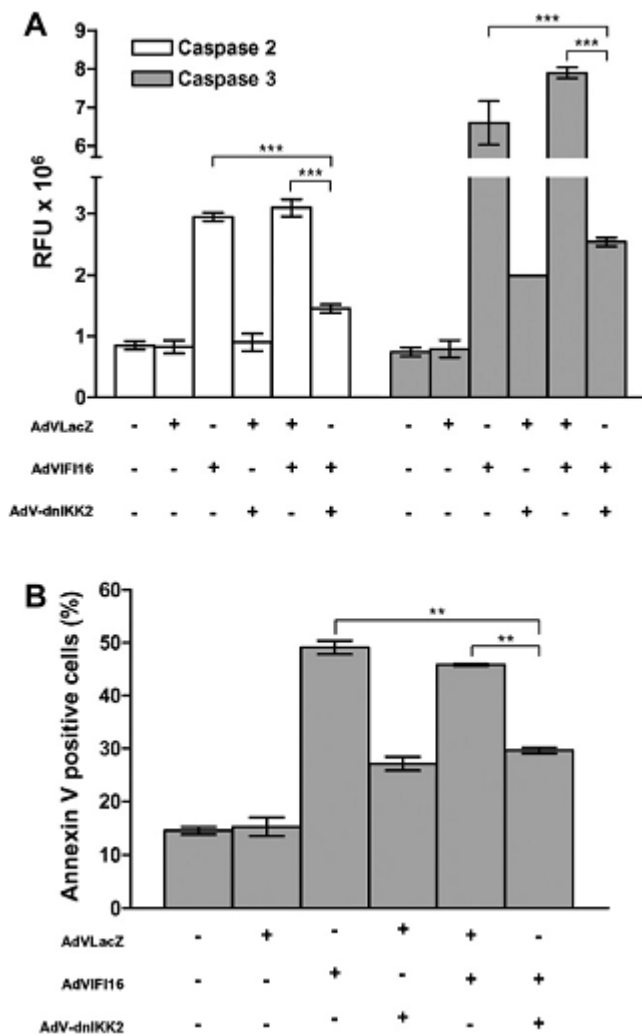


**Fig. 5.** dnIKK2 expression reduces IFI16-induced caspase activation and apoptosis. HUVEC were either single or double infected with AdVLacZ, AdVIFI16, or AdVdnIKK, or left uninfected (NI). When a double infection was performed, the second viral vector (AdVdnIKK or AdVLacZ) was added 4 h after infection with the AdVIFI16 vector. At 48 hpi, activation of caspase 2 (white bars)

and caspase 3 (grey bars) in cell extracts (A), or Annexin V-FITC binding (B) was assessed. Data are shown as mean  $\pm$  SD; n = 3. \*\*P < 0.01, \*\*\*P < 0.001 (one-way ANOVA).

To elucidate the mechanisms of IKK2 inhibition on IFI16-mediated apoptosis, we used EMSA to investigate whether the subsequent steps in the NF- $\kappa$ B activation pathway (e.g. binding to DNA), were altered by dnIKK2 expression. HUVEC were infected with AdVIFI16, AdVLacZ, or left untreated, and 4 h later infected with AdVdnIKK2. Nuclear extracts were prepared 48 hpi and evaluated for NF- $\kappa$ B binding activity. As shown in Fig. 6, strong inducible NF- $\kappa$ B activity could be detected in IFI16-overexpressing cells previously infected with AdVLacZ, whereas no significant degree of NF- $\kappa$ B activity was observed in nuclear extracts from cells infected with AdVIFI16 and then AdVdnIKK2. Notably, also induction of pro-inflammatory molecules, such as ICAM-1 and CCL20, another IFI16-induced biological activity known to depend on NF- $\kappa$ B [30], was inhibited following infection with AdVdnIKK, reinforcing the relevance of the interaction of IFI16 with NF- $\kappa$ B in triggering apoptosis (data not shown). To confirm the involvement of NF- $\kappa$ B in IFI16-induced apoptosis, we investigated the feasibility of blocking IKK2 activity using AS6022868, a low molecular weight specific inhibitor of IKK2, as a means of abrogating NF- $\kappa$ B activation and thus preventing the development of IFI16-induced apoptosis in HUVEC [32]. To avoid interfering with IFI16 expression, AS602868 (5  $\mu$ M) was only added 10 h later after the infection of HUVEC with either AdVIFI16 or AdVLacZ. Preliminary experiments confirmed that the application of 5  $\mu$ M AS602868 at this 10 h time point was able to entirely inhibit NF- $\kappa$ B activation (data not shown).

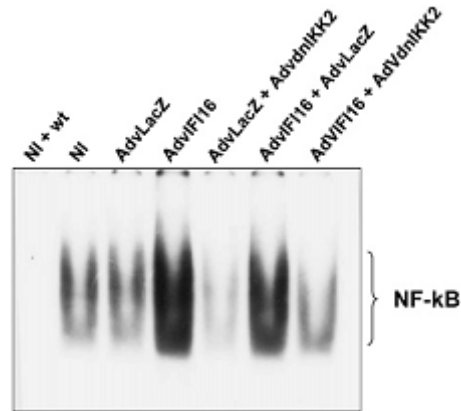


**Fig. 6.** dnIKK2 expression inhibits NF- $\kappa$ B activation HUVEC infected with AdVLacZ, AdvIFI16, or left uninfected (NI) were infected 4 h later with either AdVLacZ or AdvdnIKK. 48 hpi, nuclear extracts were prepared and analyzed by EMSA using double-stranded oligonucleotides containing NF- $\kappa$ B consensus binding sites. Each experiment was repeated at least four times, and one representative is shown.

Thus, we next measured the effect of AS602868 treatment on the ability of IFI16 to trigger the activation of caspases 2 and caspase 3. As shown in Fig. 7A, sustained IFI16 expression induced significantly higher levels of activation of both caspases in HUVEC compared to cells infected with AdVLacZ or left uninfected. In contrast, incubation of HUVEC with the NF- $\kappa$ B inhibitor 10 h after AdvIFI16 resulted in caspase activity levels that were comparable to those observed in untreated cells.

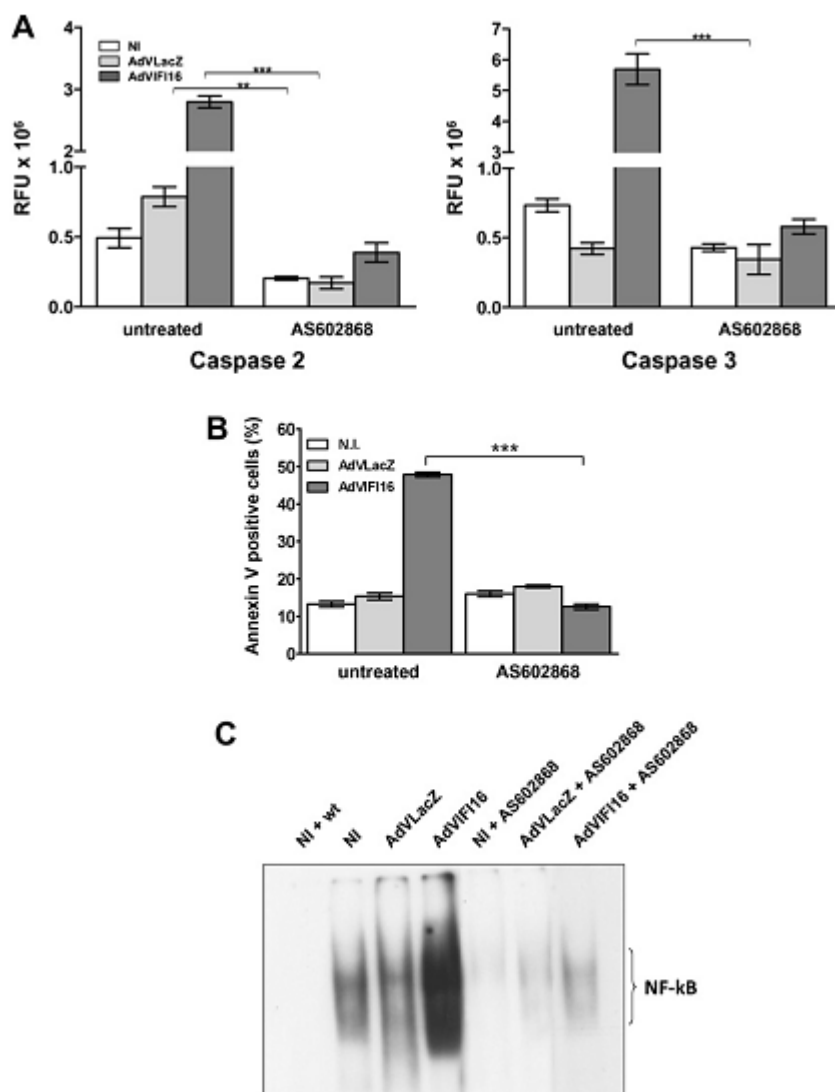


**Fig. 7.** AS602868 treatment decreases caspase activation and inhibits NF- $\kappa$ B DNA-binding activity induced by IFI16. HUVEC left uninfected (NI) or infected with either AdVLacZ or AdvIFI16 were treated 10 h later with AS602868 (5  $\mu$ M). At 48 hpi, the activation of caspase 2 and caspase 3 in cell extracts was assessed (A) and Annexin V-FITC binding (B) analyzed. C. Nuclear extracts were prepared and analyzed by EMSA using double-stranded oligonucleotides containing NF- $\kappa$ B consensus binding sites. Each experiment was repeated at least four times, and one representative is shown. Data are shown as mean  $\pm$  SD;  $n = 3$ . \*\* $P < 0.01$ , \*\*\* $P < 0.001$  (two-way ANOVA).

To assess the functional effects of NF- $\kappa$ B inhibition by AS602868 on IFI16-mediated apoptosis, HUVEC infected with either AdvIFI16 or AdVLacZ were treated with AS602868 (5  $\mu$ M) and

analyzed via Annexin V/propidium iodide FACS sorting. As expected, cultures of AdvIFI16-infected HUVEC contained 48% total apoptotic cells, a 4-fold higher percentage than that observed in cultures infected with AdvLacZ or left uninfected (Fig. 7B). In stark contrast, addition of AS602868 decreased the fraction of apoptotic cells infected with AdvIFI16 to 12%, a value comparable to that observed after AdvLacZ infection. To gain insight into the relationship of IFI16-mediated apoptosis via NF- $\kappa$ B complex activation, the effects of sustained IFI16 expression on NF- $\kappa$ B binding to its cognate DNA were examined by EMSA. As shown in Fig. 7C, nuclear extracts from both uninfected and AdvLacZ-infected HUVEC contained low levels of NF- $\kappa$ B activity. As expected, a protein–DNA complex was observed in nuclear extracts of HUVEC infected for 48 h with AdvIFI16. In contrast, treatment of AdvIFI16-infected HUVEC with AS602868 prevented the formation of this migrating DNA–protein complex, a finding consistent with the results obtained with the Annexin V/propidium iodide FACS sorting assay.

Altogether, these results demonstrate that induction of apoptosis in endothelial cells by IFI16 through caspase 2/3 activation requires functional NF- $\kappa$ B.



#### 4. Discussion

This study demonstrates for the first time that: i) IFI16 contributes in the regulation of apoptosis triggered by IFN-type I priming followed by dsRNA treatment; ii) overexpression of IFI16 in primary endothelial cells is sufficient to induce apoptosis; iii) IFI16-induced apoptosis is mediated by the simultaneous activation of caspase 2 and caspase 3; iv) activation of caspase 3 depends on caspase 2 activity, but a positive feedback loop from caspase 3 to caspase 2 may also exist; and v) the activation of caspases 2 and 3 must be mediated by the NF- $\kappa$ B complex, since the inactivation of NF- $\kappa$ B was found to prevent IFI16-induced apoptosis.

Endothelial cells, hematopoietic cells and stratified squamous epithelial cells have all been shown to express IFI16 *in vivo*, strongly suggesting that a physiological role for this protein exists in these cell types [27] and [28]. *In vitro*, immunoblotting analyses have demonstrated that IFI16 expression is barely detectable in proliferating HUVEC but that it gradually increases when cell growth halts upon the reaching of cell confluence, thus resulting in cell detachment and apoptosis [40]. Vascular involvement in autoimmune connective tissue diseases is a common complication [41] and [42]. The reduction in the number of capillaries is associated with endothelial swelling, basement membrane thickening, intima hyperplasia, along with the infiltration of inflammatory cells into the skin in several systemic autoimmune diseases. One might therefore hypothesize that the release of nuclear proteins by endothelial cells in cutaneous lesions undergoing apoptosis and necrosis may trigger the immune system and in turn bring about the production of autoantibodies. With this scenario in mind, one can envisage a role of IFI16 in systemic autoimmune diseases whereby both chronic inflammation and cell death are involved.

Caspases are a group of cysteine proteases that cleave after an aspartic acid residue at a specific recognition site [43] and [44] and the activation of these enzymes is an accepted biochemical hallmark of apoptosis. Among the 14 mammalian caspases that have been cloned to date, caspases 2, 3, 6, 7, 8, 9, 10, and 12 are the most closely involved in the apoptotic pathway; the remaining caspases have been found to be involved in the regulation of inflammatory processes. Assessing

IFI16-overexpressing HUVEC for caspase activation, only the initiator caspase 2 and the executioner caspase 3 were found to be activated. Two observations support the relevance of these two caspases in IFI16-mediated apoptosis. First, pre-treatment of HUVEC with the caspase 2-specific inhibitor Z-VDVAD-FMK or with the caspase 3-specific inhibitor Z-DEVD-FMK rendered endothelial cells resistant to apoptosis, as evaluated by measurement for their enzymatic activities and Annexin V binding. As caspase 8 is known to specifically contribute towards death-receptor signaling and as caspase 9 is activated by the apoptosome downstream of cytochrome c release by mitochondria, the lack of activation of these two caspases suggests that IFI16 specifically and solely triggers apoptosis through the activation of caspases 2 and 3.

To elucidate the mechanisms responsible for caspases 2 and 3 activation by IFI16, we adopted a genetic and a pharmacological approach to knock down either NF- $\kappa$ B or p53 function, known to be involved in apoptosis induction by various stimuli and regulatory pathways of inflammation [44], [45], [46] and [47]. Our results show that NF- $\kappa$ B, but not p53 knock down (data not shown), wiped out apoptosis. This suggests that although functional p53 might contribute in some way to the apoptotic process NF- $\kappa$ B plays a more relevant role in IFI16-mediated apoptosis. In support of these observations, we demonstrated that NF- $\kappa$ B activation is triggered by IFI16 through a novel mechanism involving the suppression of the I $\kappa$ B $\alpha$  promoter transcription accompanied by down-regulation of I $\kappa$ B $\alpha$  mRNA and protein expression. As a consequence, the NF- $\kappa$ B heterodimer, composed of p50 and p65 freely translocates into the nucleus and transactivates NF- $\kappa$ B dependent genes. Consistent with our findings, other authors have demonstrated that type I IFNs rapidly promoted NF- $\kappa$ B DNA-binding activity in diverse cell types following a progressive decrease in cellular levels of I $\kappa$ B $\alpha$ . The kinetics of induction of NF- $\kappa$ B activation paralleled those of I $\kappa$ B $\alpha$  degradation, indicating that, similar to what was observed with IFI16 overexpression, type I IFNs promote the dissociation of I $\kappa$ B $\alpha$ /NF- $\kappa$ B complexes and reduce I $\kappa$ B $\alpha$  expression [48]. Together with the finding that IFI16 silencing prevents the activation of both caspase 2 and caspase 3 by IFN-type I, these results support the physiological relevance of IFI16 as a transducer of IFN signaling.

The impact of apoptosis on immunity has been extensively investigated, and several reports suggest a correlation between apoptosis and autoimmunity through an impairment of apoptosis or an ineffective removal of apoptotic cells [9]. Furthermore, recent data have demonstrated that autoantigens are found within apoptotic bodies and that apoptotic cells are critical for the presentation of antigens, the activation of innate immunity, and the regulation of macrophage cytokine secretion [9]. A number of investigations, ranging from studies into animal models to human pathology, lend support to the view that apoptosis plays a significant role in the development of autoimmunity [6], [7], [8] and [9]. Accordingly, increased expression of IFI16 protein in skin biopsies from SSc patients has been observed [31]. Moreover, the possibility exists that environmentally-induced epigenetics changes may contribute to altered IFI16 expression in tissues from patients affected by autoimmune diseases. Increasing evidence indicates that altered patterns of DNA methylation, histone acetylation and cytosine residue methylation in CpG dinucleotides may contribute to the environment–host interaction in some forms of autoimmunity and aging [49] and [50]. Interestingly, recent studies have provided evidence that the constitutive and IFN-induced expression of IFI16 gene varies among individuals and may depend on the race and environmental factors [51], supporting the possibility that epigenetics changes may thus contribute to the increased expression of IFI16 observed *in vivo*.

In conclusion, the findings reported in this study together with our demonstration that IFI16 possesses potent pro-inflammatory activity in endothelial cells [30], provide new insights into the etiopathogenetic role of anti-IFI16 autoantibodies in patients with autoimmune diseases such as SSc, SLE, and SjS [31] and [52].

### **Acknowledgements**

We thank Howard Young for revising the manuscript. This work was supported by grants from MIUR (“PRIN 2008” to SL and MG), Regione Piemonte (“Ricerca Sanitaria Finalizzata” 2007,

2008, 2008bis and 2009 to SL, MG, MDA and MM), and Fondazione CRT (“Progetto Alfieri” to SL). PC is supported by a fellowship from Fondazione Italiana per la Ricerca sul Cancro.

## References

- [1] Degterev A, Yuan J. Expansion and evolution of cell death programmes. *Nat Rev Mol Cell Biol* 2008; 9:378-90.
- [2] Taylor RC, Cullen SP, Martin SJ. Apoptosis: controlled demolition at the cellular level. *Nat Rev Mol Cell Biol* 2008; 9:231-41.
- [3] Lang KS, Burow A, Kurrer M, Lang PA, Recher M. The role of the innate immune response in autoimmune disease. *J Autoimmun* 2007; 29:206-12.
- [4] Pisetsky DS. The role of innate immunity in the induction of autoimmunity. *Autoimmun Rev* 2008; 8:69-72.
- [5] Peng Y, Martin DA, Kenkel J, Zhang K, Ogden CA, Elkon KB. Innate and adaptive immune response to apoptotic cells. *J Autoimmun* 2007; 29:303-9.
- [6] Navratil JS, Sabatine JM, Ahearn JM. Apoptosis and immune responses to self. *Rheum Dis Clin North Am* 2004; 30:193-212.
- [7] Steinman RM, Turley S, Mellman I, Inaba K. The induction of tolerance by dendritic cells that have captured apoptotic cells. *J Exp Med* 2000; 191:411-6.
- [8] Pittoni V, Valesini G. The clearance of apoptotic cells: implications for autoimmunity. *Autoimmun Rev* 2002; 1:154-61.
- [9] Lleo A, Selmi C, Invernizzi P, Podda M, Gershwin ME. The consequences of apoptosis in autoimmunity. *J Autoimmun* 2008; 31:257-62.
- [10] Ruiz-Arguelles A, Brito GJ, Reyes-Izquierdo P, Perez-Romano B, Sanchez-Sosa S. Apoptosis of melanocytes in vitiligo results from antibody penetration. *J Autoimmun* 2007; 29:281-6.

- [11] Salunga TL, Cui ZG, Shimoda S, Zheng HC, Nomoto K, Kondo T, et al. Oxidative stress-induced apoptosis of bile duct cells in primary biliary cirrhosis. *J Autoimmun* 2007; 29:78-86.
- [12] Mandron M, Martin H, Bonjean B, Lule J, Tartour E, Davrinche C. Dendritic cell-induced apoptosis of human cytomegalovirus-infected fibroblasts promotes cross-presentation of pp65 to CD8<sup>+</sup> T cells. *J Gen Virol* 2008; 89:78-86.
- [13] Lucas M, Stuart LM, Savill J, Lacy-Hulbert A. Apoptotic cells and innate immune stimuli combine to regulate macrophage cytokine secretion. *J Immunol* 2003; 171:2610-5.
- [14] Cocca BA, Cline AM, Radic MZ. Blebs and apoptotic bodies are B cell autoantigens. *J Immunol* 2002; 169:159-66.
- [15] Koyama S, Ishii KJ, Coban C, Akira S. Innate immune response to viral infection. *Cytokine* 2008; 43:336-41.
- [16] Alsharifi M, Mullbacher A, Regner M. Interferon type I responses in primary and secondary infections. *Immunol Cell Biol* 2008; 86:239-45.
- [17] Burdick LM, Somani N, Somani AK. Type I IFNs and their role in the development of autoimmune diseases. *Expert Opin Drug Saf* 2009; 8:459-72.
- [18] Ronnblom L, Alm GV, Eloranta ML. Type I interferon and lupus. *Curr Opin Rheumatol* 2009; 21:471-7.
- [19] Asefa B, Klarmann KD, Copeland NG, Gilbert DJ, Jenkins NA, Keller JR. The interferon-inducible p200 family of proteins: a perspective on their roles in cell cycle regulation and differentiation. *Blood Cells Mol Dis* 2004; 32:155-67.
- [20] Landolfo S, Gariglio M, Gribaudo G, Lembo D. The Ifi 200 genes: an emerging family of IFN-inducible genes. *Biochimie* 1998; 80:721-8.
- [21] Luan Y, Lengyel P, Liu CJ. p204, a p200 family protein, as a multifunctional regulator of cell proliferation and differentiation. *Cytokine Growth Factor Rev* 2008; 19:357-69.

- [22] Ludlow LE, Johnstone RW, Clarke CJ. The HIN-200 family: more than interferon-inducible genes? *Exp Cell Res* 2005; 308:1-17.
- [23] Burckstummer T, Baumann C, Bluml S, Dixit E, Durnberger G, Jahn H, et al. An orthogonal proteomic-genomic screen identifies AIM2 as a cytoplasmic DNA sensor for the inflammasome. *Nat Immunol* 2009; 10:266-72.
- [24] Fernandes-Alnemri T, Yu JW, Datta P, Wu J, Alnemri ES. AIM2 activates the inflammasome and cell death in response to cytoplasmic DNA. *Nature* 2009; 458:509-13.
- [25] Hornung V, Ablasser A, Charrel-Dennis M, Bauernfeind F, Horvath G, Caffrey DR, et al. AIM2 recognizes cytosolic dsDNA and forms a caspase-1-activating inflammasome with ASC. *Nature* 2009; 458:514-8.
- [26] Roberts TL, Idris A, Dunn JA, Kelly GM, Burnton CM, Hodgson S, et al. HIN-200 proteins regulate caspase activation in response to foreign cytoplasmic DNA. *Science* 2009; 323:1057-60.
- [27] Gariglio M, Azzimonti B, Pagano M, Palestro G, De Andrea M, Valente G, et al. Immunohistochemical expression analysis of the human interferon-inducible gene IFI16, a member of the HIN200 family, not restricted to hematopoietic cells. *J Interferon Cytokine Res* 2002; 22:815-21.
- [28] Wei W, Clarke CJ, Somers GR, Cresswell KS, Loveland KA, Trapani JA, et al. Expression of IFI 16 in epithelial cells and lymphoid tissues. *Histochem Cell Biol* 2003; 119:45-54.
- [29] Raffaella R, Gioia D, De Andrea M, Cappello P, Giovarelli M, Marconi P, et al. The interferon-inducible IFI16 gene inhibits tube morphogenesis and proliferation of primary, but not HPV16 E6/E7-immortalized human endothelial cells. *Exp Cell Res* 2004; 293:331-45.
- [30] Caposio P, Gugliesi F, Zannetti C, Sponza S, Mondini M, Medico E, et al. A novel role of the interferon-inducible protein IFI16 as inducer of proinflammatory molecules in endothelial cells. *J Biol Chem* 2007; 282:33515-29.

- [31] Mondini M, Vidali M, De Andrea M, Azzimonti B, Airo P, D'Ambrosio R, et al. A novel autoantigen to differentiate limited cutaneous systemic sclerosis from diffuse cutaneous systemic sclerosis: the interferon-inducible gene IFI16. *Arthritis Rheum* 2006; 54:3939-44.
- [32] Caposio P, Musso T, Luganini A, Inoue H, Gariglio M, Landolfo S, et al. Targeting the NF-kappaB pathway through pharmacological inhibition of IKK2 prevents human cytomegalovirus replication and virus-induced inflammatory response in infected endothelial cells. *Antiviral Res* 2007; 73:175-84.
- [33] Frelin C, Imbert V, Griessinger E, Loubat A, Dreano M, Peyron JF. AS602868, a pharmacological inhibitor of IKK2, reveals the apoptotic potential of TNF-alpha in Jurkat leukemic cells. *Oncogene* 2003; 22:8187-94.
- [34] Caposio P, Luganini A, Hahn G, Landolfo S, Gribaudo G. Activation of the virus-induced IKK/NF-kappaB signalling axis is critical for the replication of human cytomegalovirus in quiescent cells. *Cell Microbiol* 2007; 9:2040-54.
- [35] Oitzinger W, Hofer-Warbinek R, Schmid JA, Koshelnick Y, Binder BR, de Martin R. Adenovirus-mediated expression of a mutant IkappaB kinase 2 inhibits the response of endothelial cells to inflammatory stimuli. *Blood* 2001; 97:1611-7.
- [36] Xin H, Pereira-Smith OM, Choubey D. Role of IFI 16 in cellular senescence of human fibroblasts. *Oncogene* 2004; 23:6209-17.
- [37] Ouchi M, Ouchi T. Role of IFI16 in DNA damage and checkpoint. *Front Biosci* 2008; 13:236-9.
- [38] Kroemer G, El-Deiry WS, Golstein P, Peter ME, Vaux D, Vandenabeele P, et al. Classification of cell death: recommendations of the Nomenclature Committee on Cell Death. *Cell Death Differ* 2005; 12 Suppl 2:1463-7.
- [39] Kaufmann SH, Lee SH, Meng XW, Loegering DA, Kottke TJ, Henzing AJ, et al. Apoptosis-associated caspase activation assays. *Methods* 2008; 44:262-72.

- [40] Panaretakis T, Laane E, Pokrovskaja K, Bjorklund AC, Moustakas A, Zhivotovsky B, et al. Doxorubicin requires the sequential activation of caspase-2, protein kinase Cdelta, and c-Jun NH2-terminal kinase to induce apoptosis. *Mol Biol Cell* 2005; 16:3821-31.
- [41] Kaiser WJ, Kaufman JL, Offermann MK. IFN-alpha sensitizes human umbilical vein endothelial cells to apoptosis induced by double-stranded RNA. *J Immunol* 2004; 172:1699-710.
- [42] Gugliesi F, Mondini M, Ravera R, Robotti A, de Andrea M, Gribaudo G, et al. Up-regulation of the interferon-inducible IFI16 gene by oxidative stress triggers p53 transcriptional activity in endothelial cells. *J Leukoc Biol* 2005; 77:820-9.
- [43] Kaplan MJ. Endothelial damage and autoimmune diseases. *Autoimmunity* 2009; 42:561-2.
- [44] Gu YS, Kong J, Cheema GS, Keen CL, Wick G, Gershwin ME. The immunobiology of systemic sclerosis. *Semin Arthritis Rheum* 2008; 38:132-60.
- [45] Kumar S. Caspase function in programmed cell death. *Cell Death Differ* 2007; 14:32-43.
- [46] Logue SE, Martin SJ. Caspase activation cascades in apoptosis. *Biochem Soc Trans* 2008; 36:1-9.
- [47] Cuenin S, Tinel A, Janssens S, Tschopp J. p53-induced protein with a death domain (PIDD) isoforms differentially activate nuclear factor-kappaB and caspase-2 in response to genotoxic stress. *Oncogene* 2008; 27:387-96.
- [48] Haupt S, Berger M, Goldberg Z, Haupt Y. Apoptosis - the p53 network. *J Cell Sci* 2003; 116:4077-85.
- [49] Shishodia S, Aggarwal BB. Nuclear factor-kappaB activation: a question of life or death. *J Biochem Mol Biol* 2002; 35:28-40.
- [50] Du Z, Wei L, Murti A, Pfeffer SR, Fan M, Yang CH, et al. Non-conventional signal transduction by type 1 interferons: the NF-kappaB pathway. *J Cell Biochem* 2007; 102:1087-94.



- [51] Mondini M, Vidali M, Airo P, De Andrea M, Riboldi P, Meroni PL, et al. Role of the interferon-inducible gene IFI16 in the etiopathogenesis of systemic autoimmune disorders. *Ann N Y Acad Sci* 2007; 1110:47-56.